ELSEVIER

Thin Solid Films 303 (1997) 255–263

thin solid films

A method for monitoring the thickness of semiconductor and dielectric thin films: application to the determination of large-area thickness profiles

Y. Laaziz [a,*], A. Bennouna [a], M.Y. Elazhari [a], J. Ramiro-Bargueño [b,1], A. Outzourhit [a], N. Chahboun [a], E.L. Ameziane [a]

[a] *L.P.S.C.M, Faculté des Sciences Semlalia, Dépt. Physique, B.P. S / 15, 40000 Marrakech, Morocco*
[b] *UAM, Facultad de Ciencias, Dto. Fisica Aplicada C-XII, 28049 Madrid, Spain*

Received 13 May 1996; accepted 16 January 1997

Abstract

We report here a method for determining the thickness of semiconductor and dielectric thin films based on the optical transmission turning points. An analytical treatment of the transmittance taking into account the shrinkage of the interference fringes caused by thickness inhomogeneities and the bandwidth of the incoming radiation is used. The computation algorithm is original, simple and straightforward. The accuracy of the method is studied, and the effects of the experimental noise, the uncertainty in the value of the substrate refractive index and of the number of available fringes on the spectra are considered. The precision of the thickness is estimated to be around 0.4% (or less) for films whose optical thicknesses (product of the refractive index and the thickness) are in the range 0.5–10 μm. The method is applied to obtain large-area thickness profiles by computing the thickness from spectra taken over different positions of the film surface. In this case, a special mechanical mounting is needed for the acquisition of the transmission data. This procedure presents the advantage of local analysis of the films, allowing the non-flatness of the substrate to be ignored. This last is the major inconvenience in the use of a surface profile measurement system. Results are given for films up to 7 cm large (there is no difficulty in increasing this value even further) and with different thickness profiles. © 1997 Elsevier Science S.A.

Keywords: Dielectrics; Optical properties; Semiconductors; Surface defects

1. Introduction

Accurate measurements of the thickness of semiconductor and dielectric thin films are of great importance, not only at the industrial scale, particularly for optical coatings and photo-optical devices, but also at the laboratory scale where the thickness is always required as an input parameter for other physical characterizations, as well as for the calibration of growth rates or monitoring thickness uniformity.

The thickness can be controlled in-situ, using e.g. a quartz crystal oscillator, but in most cases the measurements are performed after deposition. Several techniques exist for this purpose [1], but the most common ones are the spectrophotometric methods, particularly the spectral normal transmittance (T) or the spectral near-normal specular reflectance (R) owing to their simplicity and the availability of the equipment required. In fact, unless the film surface is too rough or the film is highly inhomogeneous, the T and R spectra of semiconductor and dielectric thin films in the region of transparency contain interference patterns whose shapes depend on the thickness t and refractive index $n(\lambda)$ of the film. These two parameters, together with the imaginary part of the refractive index $k(\lambda)$, can be found independently from either of these spectra, and without prior knowledge of any of the film characteristics. This mathematically insoluble problem (N equations and $2N+1$ unknowns) finds its solution using the envelopes of the interference pattern, considered as continuous functions of λ, and the fringe positions. This is the well-known turning point (or envelope) method, as it was first proposed by Manifacier [2] using the spectral

* Corresponding author. Fax: +212 443 6769; e-mail: bamin@onpt.net.ma.

[1] Also at the: Universidad de Navarra, Facultad de Ciencias, Departamento de Física y Matemática Aplicada, 31080, Pamplona, Spain.

PII S0040-6090(97)00044-8

transmittance. However, it has been demonstrated elsewhere [3–5] that this method can lead to serious errors in the determination of the optical constants and the thickness if the geometrical and structural inhomogeneities of the film (e.g. surface roughness, continuous thickness variation, refractive index variation, etc.), as well as the experimental non-zero bandwidth, are not taken into account. So, in using this method, a correct procedure must necessarily take into account all, or at least the most important effects which influence the T and R spectra. Nevertheless, finding simple analytical expressions for T or R in the presence of more than one type of inhomogeneity inside the film is a difficult mathematical task. But when a given kind of inhomogeneity predominates over the others, it is possible to find, via some justified physical assumptions, simple analytical expressions for T [5] and R [6], which can be easily solved to an excellent precision for $n(\lambda)$, $k(\lambda)$ and t. In addition, one can also obtain an estimate of the magnitude of this inhomogeneity [4].

From a practical point of view, transmittance data are usually preferred to reflectance data because the measurements are more accurate and straightforward. In addition, they are less sensitive to surface inhomogeneities, which explains why most major work in this field has been done using the transmittance [2–5,7,8]. To our knowledge, little work [9,10] has been devoted to the extraction of the optical constants and thickness from reflectance measurements.

Swanepoel [3] was the first to report analytical expressions for the transmittance of transparent thin films presenting thickness or index fluctuations over the illuminated area, but this required the use of three absorption regions. In previous work using the transmittance inverse [5], we developed a theoretical analysis of the transmission of semiconductor thin films in the presence of such inhomogeneities, which yielded a more simplified and unique analytical expression for the transmittance standing over the entire spectrum. We also treated the bandwidth effect and presented a method for computing the optical constants, thickness and degree of thickness or index inhomogeneities in the films based on the resulting equations. Other workers [4] used experimental spectra from films having a continuous thickness variations as a principal inhomogeneity to confirm the most relevant features of the analytical formalism in this special case. The advantages of our version of the turning point method over other reported procedures can be summarized as follows:

- A unique and simple analytical expression of the transmittance, taking into account the presence of inhomogeneities and the finite bandwidth, is used over the entire spectrum.
- The reflection of a rough surface is introduced in the transmittance formula to take into account the beam scattering losses at the top interface when the film is thought to have a pronounced surface roughness (as in polycrystalline or polymer thin films) [5].
- A nonlinear least-squares smoothing of the experimental spectrum is performed to reduce the noise in the experimental apparatus; this enhances the precision of the determination of the turning point wavelength positions.
- The fringe orders are determined in a straightforward manner without the need for any iterative computations.
- The envelope curves are computer-drawn using a nonlinear interpolation; this enhances the precision of the determination of the fringe contrast.
- A time-saving original computation algorithm is used and the program is fully graphic.

Given the excellent precision to which the thickness can be computed (around 0.4% or less), we show an original way to make thickness profiles for large-area thin films. In fact, when the analyzed region extends beyond a few centimeters, thickness profiles can not be correctly performed using a stylus profilometer due to the inherent artifacts caused by the non-flatness of the substrate, which is usually of the same order of magnitude as the actual film thickness. The advantage of this spectrophotometric method resides in the local nature of the analysis of the sample, thus enabling the non-uniformity of the substrate thickness not to be "seen" by the incident beam. These measurements are of interest at the laboratory scale, particularly in the optimization of the growth conditions for better thickness homogeneity. As is well known, the film thickness distribution depends on many factors, such as the method of deposition, the dimensions and shape of the deposition chamber, and the position of the substrate with respect to the source [11]. The thickness profile measurements give an exact idea of the shape of the deposits for a given set of deposition conditions.

2. Theoretical background

2.1. Film free of thickness inhomogeneities

A monochromatic beam is incident normally on a film of complex refractive index $\tilde{n} = n - ik$ and thickness t deposited on a non- absorbing substrate. If we assume smooth and parallel interfaces and multiple reflections to be coherent in the film and incoherent in the substrate, the transmission inverse is given by [12–14]

$$\frac{1}{T} = \frac{\left[e^{\alpha t} + R_{10}R_2 e^{-\alpha t}\right]\left[1 - R_2R_3A^2\right]}{(1-R_{10})(1-R_2)(1-R_3)A} + \frac{2\sqrt{R_{10}R_2}\left[1 - R_2R_3A^2\right]}{(1-R_{10})(1-R_2)(1-R_3)A}\cos(\chi) \quad (1)$$

or

$$\frac{1}{T} = I_F(R_{10}, R_2, R_3, \alpha, t) + g(R_{10}, R_2, R_3)\cos(\chi) \quad (2)$$

where

$$\chi = \delta_1 + \delta_2 - \varphi = \delta_1 + \delta_2 - \frac{4\pi nt}{\lambda} \quad (3)$$

where R_{10}, R_2 and R_3 are the normal reflectances at the air–film, film–substrate and substrate–air interfaces, respectively, δ_1 and δ_2 are the phases of the Fresnel reflection coefficient at the air–film and film–substrate interfaces, respectively, $\alpha = 4\pi k/\lambda$ is the absorption coefficient, and A is an attenuation term taking into account eventual absorption in the substrate (in our case $A \simeq 1$).

Our preference to work with the transmittance inverse is dictated by the simplicity of the analytical treatment of the obtained formula: the oscillating and non-oscillating parts of the transmittance become algebraically separated; and as pointed out in Section 1, we do not have to consider three absorbing spectral regions to solve our equations [3,7,8].

In the following we assume that the film–substrate and substrate–air interfaces are perfectly smooth and parallel.

2.2. Film including a continuous thickness variation

If the film presents a thickness variation of a very low slope over the illuminated area, and if σ is the maximum departure from the average thickness, it has been demonstrated that a correction term appears in Eq. (2) [5,4], and the new expression for the transmittance inverse is given by

$$\frac{1}{T} = I_F(R_{10}, R_2, R_3, \alpha, t) + g(R_{10}, R_2, R_3) \times \left[\frac{\sin \Delta\varphi}{\Delta\varphi}\right] \cos(\chi) \quad (4)$$

where $\Delta\varphi = 4\pi n\sigma/\lambda$ is the phase fluctuation due to the thickness fluctuation σ.

2.3. Bandwidth effect

In practice the spectrophotometer has a finite bandwidth $\Delta\lambda$ set by the entrance and exit slits of the instrument. Consequently, a band of wavelengths between $(\lambda - \Delta\lambda)$ and $(\lambda + \Delta\lambda)$ is incident on the sample. Taking into account the bandwidth value $\Delta\lambda$ in the analytical treatment, another correction term appears in Eq. (4), and the transmission inverse becomes

$$\frac{1}{T} = I_F(R_{10}, R_2, R_3, \alpha, t) + g(R_{10}, R_2, R_3) \times \left[\frac{\sin \Delta\varphi}{\Delta\varphi}\right] \left[\frac{\sin\left(\frac{4\pi nt\Delta\lambda}{\lambda^2}\right)}{\frac{4\pi nt\Delta\lambda}{\lambda^2}}\right] \cos(\chi) \quad (5)$$

which can be written as

$$\frac{1}{T} = I_F(R_{10}, R_2, R_3, \alpha, t) + \frac{C}{2}\cos(\chi) \quad (6)$$

where

$$C = 2g(R_{10}, R_2, R_3)\left[\frac{\sin \Delta\varphi}{\Delta\varphi}\right]\left[\frac{\sin\left(\frac{4\pi nt\Delta\lambda}{\lambda^2}\right)}{\frac{4\pi nt\Delta\lambda}{\lambda^2}}\right] \quad (7)$$

is the fringe contrast for a given wavelength.

In summary, it can be said that thickness inhomogeneities and the non-zero bandwidth result in a shrinkage of the interference pattern, without altering the non-oscillating part of the transmittance inverse (I_F).

Expressions identical to Eq. (5) are obtained when we consider films that present lateral refractive index variations or surface roughness. For the former, the transmittance inverse is obtained by changing the phase fluctuation $\Delta\varphi = 4\pi n\sigma/\lambda$ by $\Delta\varphi' = 4\pi(\Delta n)t/\lambda$, where Δn is the maximum variation of the refractive index from the average value. For the latter, a reflection R_1 of a rough surface must be considered, $\Delta\varphi$ being unchanged. For complete details of the theoretical formalism, see Ref. [5].

As noted in Section 1, the computed values of σ and Δn can have a significant physical meaning only when they are known, via some independent characterization, to be individually the predominant inhomogeneity in the film. For example, we have been able to estimate to good accuracy the value of the thickness variation σ over the illuminated area for a film presenting a high degree of thickness variation [4]; in this case the film thickness profile had been obtained previously. When no additional information is available on the studied film, and if only the determination of the film thickness is of interest (as in the present work), any of the three proposed models can be used. This is because the convergence criterion in our computations is the minimization of the difference between experimental and computed contrasts (see the algorithm in Fig. 2) and this can be achieved using σ or Δn as the fitting parameters.

3. Thickness determination

3.1. Transmission data acquisition

The transmission spectra are obtained using a Shimadzu 3101PC UV–VIS–NIR double-beam spectrophotometer fitted with a data acquisition station. All the usual and necessary precautions are taken during data acquisition [4]. Typically, the size of the light spot on the films is fixed at around 1×5 mm^2 and the experimental bandwidth $\Delta\lambda$ is kept automatically at 2 nm. The relative uncertainty in the transmittance given by the manufacturer is 0.2% [15].

Transmission scans are performed using a constant wavelength step (2 nm) and without a substrate in the reference compartment. The spectra are then normalized with respect to the substrate transmittance. The resulting spectra are subsequently smoothed to eliminate the residual noise (especially at high wavelengths) by a nonlinear least-squares fit. This is followed by converting them into spectra with a constant energy step (5 meV) by polynomial interpolation.

3.2. The substrate refractive index

In most cases, the glass spectral refractive index can be found in optics handbooks [16]. In our case, the substrate refractive index n_s is obtained from its normal transmittance T_s, which is given by [12–14]

$$T_s = \frac{2n_s}{1+n_s^2} \tag{8}$$

The relative uncertainty in n_s depends strongly on the optical quality of the glass substrate; the existence of weak absorption bands in the substrate transmittance makes the estimation of n_s more inaccurate due to the non-flatness of T_s. For Corning glass we have estimated this uncertainty to be around 0.2%; for other types of glass it is around 0.5%.

3.3. The envelopes

The positions of the extrema are automatically detected within a user-defined confidence interval (usually 5 or 7 experimental points). A few fringes located near the absorption threshold appear as weak oscillations in the transmittance. Their positions are obtained from the second derivative of the spectrum. For the thickness computations we generally consider the high wavelength region where the fringes are well contrasted. In this case, the use of fringes near the absorption region is imposed when the spectrum contains only a few fringes. Nevertheless, the uncertainty in the thickness may become slightly higher, as will be shown in Section 4.

The spectral envelopes of the transmittance, $T_{max}(\lambda)$ and $T_{min}(\lambda)$, which are assumed to be continuous functions of the wavelength, are computed using a polynomial interpolation between extrema in which the continuity of the function and its first derivative are imposed at both sides of an extremum. An example of the computed envelopes is shown in Fig. 1 for an a-Si thin film.

Considerable time can be saved if the spectral envelopes are computer drawn. In fact, this enables the process of determining the thickness and optical constants to be fully computerized. In addition, the precision of the determined parameters is enhanced.

3.4. The fringe contrast

Once the envelopes are computed, the transmission spectrum is reduced to the wavelengths λ_i at which the fringe extrema have been detected. Then, the experimental contrasts are calculated,

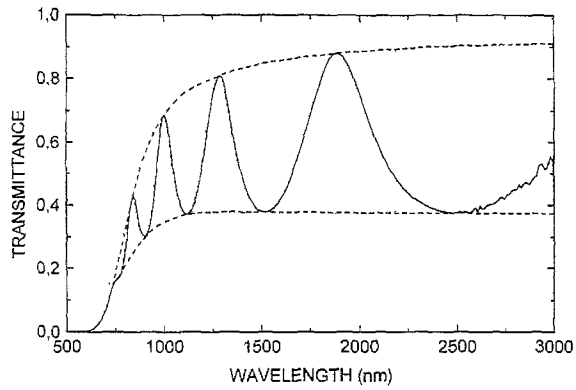

Fig. 1. Example of the computed transmittance envelopes for an a-Si thin film.

$$C(\lambda_i) = \frac{1}{T_{min}(\lambda_i)} - \frac{1}{T_{max}(\lambda_i)} \tag{9}$$

The fringe contrast is used to get a first estimation of the refractive indices $n(\lambda_i)$ since the former depends only on the refractive index, when the effect of thickness inhomogeneities and bandwidth are omitted (see Eqs. (5) and (6)).

3.5. The optical thickness

The optical thicknesses $D(\lambda_i)$ are deduced from the wavelength positions λ_i at which the interference condition holds:

$$D(\lambda_i) = n(\lambda_i)t = (p+i-1)\lambda_i/4 \tag{10}$$

where i is a variable integer assigned to the fringes according to their positions in the interference pattern. It is counted from the rightmost fringe in the wavelength axis, and p is a fixed integer, which represents the order of the first fringe ($i = 1$). p is even for transmission maxima and odd for minima when $n > n_s$ [14]. Hence, knowledge of p gives the optical thickness at each fringe position.

3.5.1. Case of availability of the refractive index tail

A first estimate of p is given by the integer of appropriate parity nearest to $\lambda_2/(\lambda_1 - \lambda_2)$. In most cases, this has proven to give the exact solution if the fringes used are in the long-wavelength tail of the refractive index. The correctness of this value is later tested qualitatively. In fact, the spectral behavior of the refractive indices for semiconductors and dielectrics can be fitted by the one-oscillator Sellmeier dispersion law [17], so that the optical thickness can be expressed in the same way:

$$D^2(\lambda) = (n(\lambda).t)^2 = (n_\infty.t)^2 + \frac{(b.t)^2}{\lambda^2 - \lambda_0^2}$$

$$= D_\infty^2 + \frac{B^2}{\lambda^2 - \lambda_0^2} \tag{11}$$

where n_∞ is the IR-extrapolated refractive index, λ_0 is the characteristic wavelength of the oscillator, and b is a constant.

Eq. (11) shows that the optical thickness tends towards a roughly stationary value D_∞ when λ increases (NIR wavelengths). It can also be readily verified that only the exact order gives to the determined $D(\lambda_i)$ a shape which is consistent with Eq. (11). An erroneous estimate of p yields an optical thickness with an upward trend at high wavelengths if p is overestimated, and with a downward trend in the opposite case. Following this method, one can confirm or change the order of the first fringe so as to fit the calculated $D(\lambda_i)$ with the physically known spectral behavior of the optical thickness (see Ref. [2]).

3.5.2. Case of absence of the refractive index tail

This is the case of equipment operating at wavelengths below 0.9 μm, especially when they are used to characterize narrow band-gap semiconductors. Here, the approximation $p \simeq \lambda_2/(\lambda_1 - \lambda_2)$ is no longer acceptable due to the dispersion in the refractive index. It is then necessary to have an exact idea of the optical thickness of the film. This is not so restrictive; in fact, the error introduced in the optical thickness for the ith fringe by considering successive wrong orders can be written as

$$D_q(\lambda_i) - D_{q\pm 2n}(\lambda_i) = n\frac{\lambda_i}{2} \tag{12}$$

where q denotes the correct order corresponding to this fringe, and $q \pm 2n$ denotes the incorrect ones; n is an integer ($n = 1, 2, 3, \ldots$). Assuming $\lambda_i = 800$ nm, this difference for two orders adjacent to the real one (orders $q \pm 2$) is 400 nm. It is sufficiently high that a rough estimate of the film optical thickness (around 10%, for example) allows us to find out the exact order. To do this, one could measure an approximate thickness using a Michelson interferometer or an edge profilometer, and take the refractive index from the literature.

3.6. Computations

With N experimental fringes, we have N equations given by the optical thickness $D(\lambda_i)$; N equations given by $\{1/T_{max}(\lambda_i) + 1/T_{min}(\lambda_i)\}/2$; and N others given by the experimental contrasts $C(\lambda_i)$. This leads to $3N$ equations and only $2N + 2$ unknowns, $n(\lambda_i)$, $\alpha(\lambda_i)$, t and σ. The problem is resolved in a statistical manner according to the algorithm given in Fig. 2. The results (t and $n(\lambda)$) are obtained after 5–7 runs of the program loops. This takes less than a minute using an IBM-486 computer.

The technique has been applied to the optical characterization of thin films of various families of compounds:

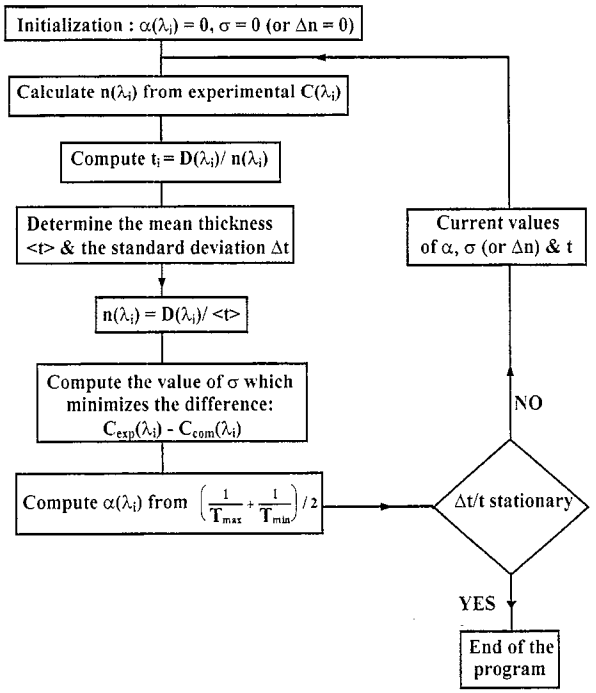

Fig. 2. The computation algorithm.

amorphous [18,21], polycrystalline [22,23], and polymers [24].

4. Error analysis

The accuracy of the proposed method depends on the following factors:

- The number of available fringes on the spectra: since the final thickness is the average value over the thicknesses obtained at each fringe position, the accuracy of t should be enhanced with increasing numbers of fringes and vice versa.
- The fringe wavelengths have to be as precise as possible: with a recent digital spectrophotometer and good algorithm using a local polynomial smoothing, we have no difficulties from this point of view.
- The experimental noise in the spectra can influence the exact determination of the fringe positions and contrasts.
- The precision of the estimate of the substrate refractive index: this has been discussed in Section 3.1.
- The magnitude of the fringe contrast: this is an increasing function of the difference between the film and substrate refractive indices. In Fig. 3 we show a plot for a given wavelength of the relative error in n versus this difference, for four levels of uncertainty in the computations of the fringe contrast. It is clear that the errors in n and consequently in t (see the algorithm of Fig. 2) are important for films with refractive indices close to that of the substrate (i.e. dielectric films).

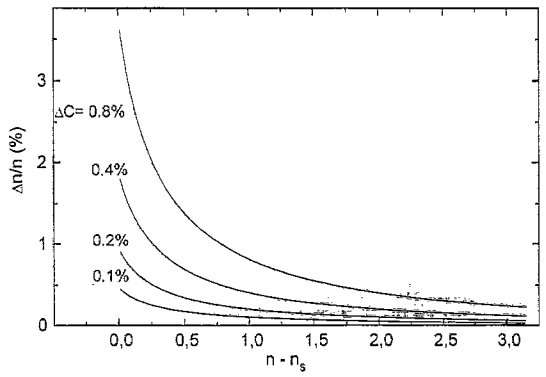

Fig. 3. Relative error in the refractive index versus the difference $n - n_s$ for four levels of error in the computation of the contrast.

In what follows the influence of all these factors will be studied. For this purpose, we suppose a dielectric thin film (low contrast) deposited on a transparent substrate of real refractive index $n_s = 1.51$. The film has the following characteristics: refractive index

$$n(\lambda) = \sqrt{(1.75)^2 + \frac{(0.4)^2}{\lambda^2 - (0.35)^2}} \quad (\lambda \text{ in } \mu\text{m})$$

absorption coefficient

$$\alpha(\lambda) = 1.54 \times 10^5 \, e^{-10^3(\lambda - 0.34)^2} \quad (\lambda \text{ in } \mu\text{m})$$

average thickness t, and thickness variation $\sigma = 25$ nm.The values of $n(\lambda)$ and $\alpha(\lambda)$ represent typical empirical equations obtained for dielectric thin films such as In_2O_3, SnO_2, ZnO, etc.

Using this model system and Eq. (5), in which we took $\Delta\lambda = 2$ nm, a set of transmittance spectra were computed by varying the average thickness. This allowed us to vary the number of available fringes on the spectra (N). 0.2% noise was added to the spectra so that they more closely resembled the experimental ones. Fig. 4 shows a comparison of an experimental interference pattern corresponding to a ZnO sputtered film and that of a computed spectrum. The noise in the experimental spectrum is lower than that in the computed one. It can therefore be said that the value

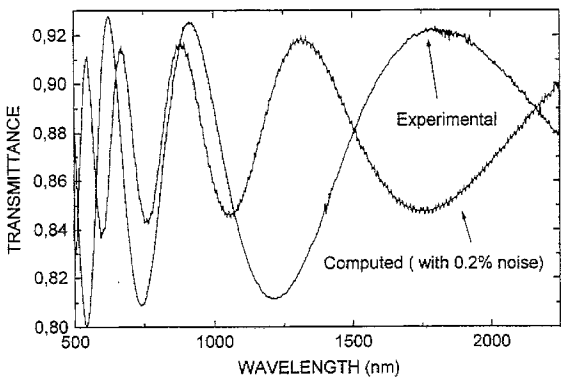

Fig. 4. Comparison of experimental and computed spectra.

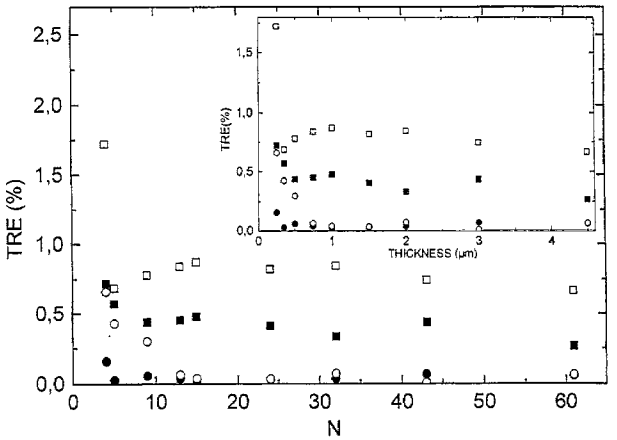

Fig. 5. TRE as a function of N: ● (0%, 0%), ○ (0.2%, 0%), ■ (0.2%, 0.5%), □ (0.2%, 1%) (the first percentage refers to the level of noise in the computed spectra, and the second to the error in n_s assumed for the computations).

of 0.2% noise assumed in the computation is somewhat overestimated.

The procedure described above was used to determine the thicknesses of each of the computed spectra. The results are shown in Fig. 5, where we have plotted the thickness relative error (TRE) as a function of N and as a function of the thickness for the inserted figure. We have also studied the effect of a hypothetical error in n_s on the computed thickness. The results of this study are also shown in Fig. 5 for two overestimates of n_s: $n_s + 0.005n_s$ and $n_s + 0.01n_s$.

From an analysis of Fig. 5 we conclude that for computed spectra without additional noise the TRE is lower than 0.1% if $N > 4$; the addition of 0.2% of noise in the spectra has no influence on the TRE except for low values of N, especially for $N = 4$; and the uncertainty in the refractive index of the substrate (n_s) increases the values of the TRE to around 0.4% and 0.8% for errors in n_s of 0.5% and 1%, respectively.According to this analysis, and taking account of the experimental relative error in the determination of n_s which we overestimate to be 0.5%, we can locate the precision of the method to $\lesssim 0.4\%$ if the thickness (in fact, the optical thickness) is sufficiently high to yield to more than four spectral fringes. This constraint fixes a lower limit on the optical thickness for the application of the method at an estimated value of 0.6 μm. The upper limit (around 10 μm) is fixed by the partial incoherence of the incident light when the fringe order increases [5].

5. Thickness profiles

5.1. Principle of the method

In the region where $k/n \ll 1$, if $n > n_s$, it can be shown that $\delta_1 + \delta_2$ is close to π, so the interference

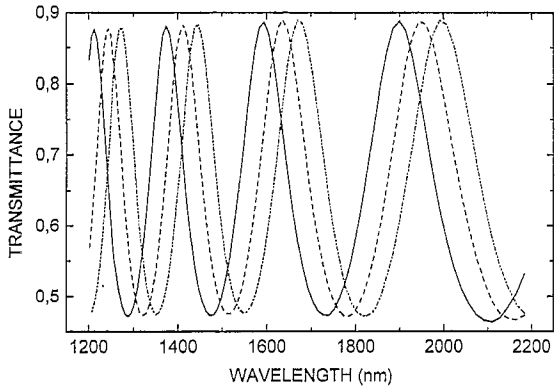

Fig. 6. Set of experimental interference patterns showing the shifts in the wavelengths of the fringes of equal order when regions of different optical thicknesses are analyzed.

fringes are practically periodic in $4\pi n(\lambda)t/\lambda$. Therefore, a slight variation in the optical thickness at a given λ, from one position in the film to another, must lead to a change in the transmittance. This is manifested, when taking spectra from regions of different optical thicknesses, by a displacement in the wavelengths at which the fringe extrema occur. A fringe of a given order is shifted to higher wavelengths if the optical thickness increases and vice versa. Zero displacement of the fringes reveals that the film is optically homogeneous over the analyzed region. As an example, Fig. 6 shows a set of experimental transmittance spectra obtained when analyzing sample 1 (see Table 1). We can note the shift of the fringes when the analysis is performed going from the edge (lower thickness) to the central position of the sample (higher thickness). This simple property of the spectral characteristics of the transmission, together with the procedure of thickness determination described above, are used in what follows to obtain the thickness profiles.

5.2. Technical procedure

The sample is fixed vertically on a mounting as shown in Fig. 7. This accessory is incorporated in the analysis chamber of the spectrophotometer. The mounting enables the sample to be moved both vertically and horizontally. For our measurements only horizontal displacements of the sample are performed.

Transmittance spectra are first acquired at the edge of

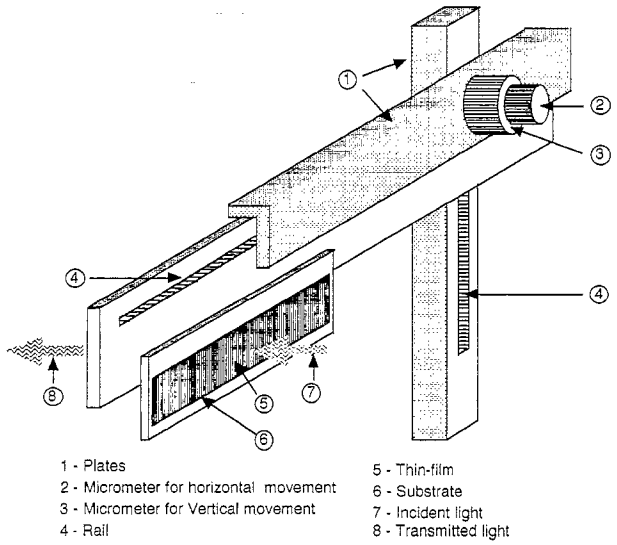

Fig. 7. Simplified scheme of the mounting used for the accurate movement of the sample in front of the spectrophotometer light spot. Spectra are taken from different positions all over the sample with a fixed distance between positions to make a thickness profile.

the sample (position 0) and then at successive positions separated by a fixed distance. This distance can be chosen conveniently (16/9 mm in our case). The explored positions are estimated to be known to better than 0.3 mm. The thickness at each analyzed position is found from the analysis of the corresponding transmission spectrum using the procedure described in Section 3.

5.3. Samples

Samples of different materials (a-Si, a-Si:H, CdTe) grown by radio-frequency sputtering were used for illustrative purposes. Their growth conditions are given in Table 1. The sputtering chamber has stainless steel walls and is equipped with three circular water-cooled cathodes 10 cm in diameter. Other details can be found in a previous paper [25].

5.4. Results

Fig. 8 shows the thickness profiles obtained for samples 1, 2 and 3. We remark that the region of thickness

Table 1
Deposition parameters for the illustrated thin films

Sample	Nature of deposit	Rf power (W)	Argon partial pressure (mbar)	Hydrogen partial pressure (mbar)	Substrate temperature (°C)	Substrate–target distance (cm)
1	a-Si:H	250	10^{-2}	5×10^{-4}	200	6
2	CdTe	175	3×10^{-2}	0	25	6
3	CdTe	250	3×10^{-3}	0	25	6
4	a-Si	250	10^{-2}	0	25	Varying [a]
5	a-Si	250	10^{-2}	0	25	Varying
6	a-Si	250	10^{-2}	0	25	Varying

[a] See Section 5.4 for details.

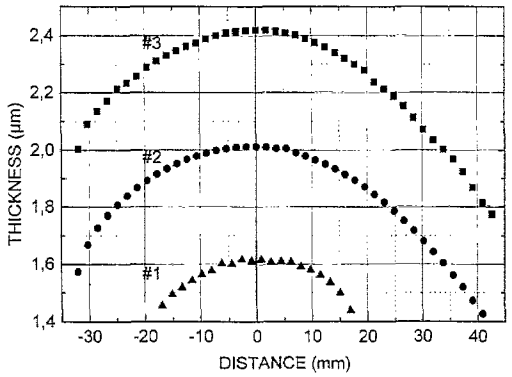

Fig. 8. Thickness profiles obtained for samples 1, 2 and 3.

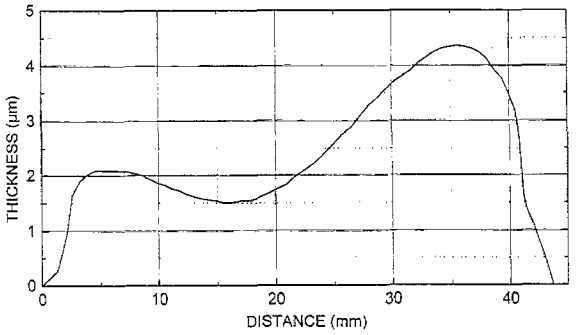

Fig. 10. Thickness profile obtained for sample 1 using a surface profilometer.

homogeneity is limited to a small area of less than 2 cm around the target axis. We also obtained analogous profiles for sputtered V_2O_5 films [19,20]. Fau et al. reported similar shapes for sputtered MnO_4 films [26]. In their case the thickness profiles were obtained by measuring the thickness (using a surface profilometer) independently from different samples placed at positions around the target axis during deposition. The thickness distribution observed for sputtered materials was predicted by Nanbu et al. [27] using a Monte Carlo simulation of the growth rate. These authors demonstrated that films of uniform thickness can not be achieved with a uniform erosion distribution of the target.

Fig. 9 shows the thickness profiles obtained for samples 4, 5 and 6. The straight lines are the least-squares fits of the experimental values (symbols). The agreement between the experimental profiles and the corresponding linear fits is sufficiently good to qualify the films as wedge-shaped. In fact, such thickness variations were made intentionally in order to test the method with different profiles. This was done by placing the substrates in an oblique position in front of the target, allowing the deposition rate to vary from one edge of the sample to the other.

Attempts were made to obtain the thickness profiles using a surface profilometer, but this led to erroneous results because of the non-flatness of the substrate which appears systematically when a wide area (a few centimeters, for example) is analyzed. As an example, Fig. 10 shows the profile obtained for sample 1 using a Sloan DEKTAK 3030 surface profilometer. Special care was taken to analyze the same region of the sample as that characterized optically (Fig. 8). We note that the non-flatness of the substrate surface masks the actual shape of the film thickness; in addition, the maximum profiled thickness is about three times higher than the actual one.

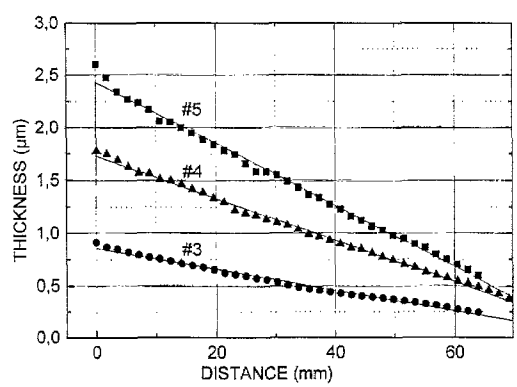

Fig. 9. Thickness profiles obtained for samples 4, 5 and 6. The straight lines are the least-squares fits of the experimental values.

5.5. Comments

It may be thought that the proposed thickness profile method is time-consuming because of the numerous transmittance spectra that are needed. However, considerable time can be saved by measuring the spectra only over the spectral region of interest, i.e. the oscillating part of the transmittance used to find the thickness, or by increasing the distance between contiguous explored positions when the analyzed samples are too large. Another way to save time is to treat only one spectrum when the transmittances from different regions are identical. This occurs when the analyzed regions have the same thickness.

When the refractive index of the film is not dependent on the growth rate, which may change from an edge to a center of the film, as shown for sputtered films (see Fig. 8), the procedure becomes even simpler. In this case, only one spectrum must be carried out and treated using the method of Section 3, to determine the corresponding thickness t and the spectral refractive index $n(\lambda)$ obtained by fitting $n(\lambda_i) = [D(\lambda_i)/t]$ by the Sellmeier dispersion law [17]. To profile the film thickness, one should select a fringe of known order from the previously obtained spectrum and follow the shift in the x-axis of the corresponding wavelength λ_i with changing position over the film (see Fig. 6). The thickness is determined using Eq. (10). With the new generation of equipment this can be done directly on the computer screen.

6. Summary

The turning point method is widely used for monitoring the thickness of semiconductor and dielectric thin films. In this work we have shown that the combination of a rigorous theoretical analysis, precision in the data acquisition and treatment, and an improved computation algorithm give the thickness with an excellent accuracy. In some unfavorable conditions (low fringe contrast, 0.5% error in n_s, 0.2% noise in the transmittance and only five spectral fringes), the error is estimated to be around 0.4%. This result is of great interest given the simplicity of the method and the availability of the equipment required.

The application of the method to profile some relatively large-area thin films with two different kinds of thickness inhomogeneity — convex-shaped and wedge-shaped thickness variations — has given very satisfactory results and has proven its efficiency in overcoming the difficulties caused by the non-flatness of the substrate, which is the main inconvenience in the use of a surface profilometer in this regard.

Acknowledgements

This work was partly supported by the bilateral agreement between the Universidad Autonoma de Madrid and the Cadi Ayyad University and the MedCampus Program (Network #15) of the European Community.

References

[1] A. Piegari, E. Masetti, Thin Solid Films 124 (1985) 249.
[2] J.C. Manifacier, J. Gasiot, J.P. Fillard, J. Phys. E: Sci. Instrum. 9 (1976) 1002.
[3] R. Swanepoel, J. Phys. E: Sci. Instrum. 17 (1984) 896.
[4] Y. Laaziz, A. Bennouna, Thin Solid Films 277 (1996) 155
[5] A. Bennouna, Y. Laaziz, M.A. Idrissi, Thin Solid Films 213 (1992) 55.
[6] Y. Laaziz, M. Benmoussa, A. Bennouna, in preparation.
[7] P. Meredith, G.S. Buller, C. Walker, Appl. Opt. 32 (1992) 5619.
[8] M. Nowak, Thin Solid Films 254 (1995) 200.
[9] D.B. Kushev, N.N. Zheleva, Y. Demakopoulou, D. Siapkas, Infrared Phys. 26 (1986) 385.
[10] D.A. Minkov, J. Phys. D: Appl. Phys. 22 (1989) 1157.
[11] Sh.A. Furman, A.V. Tikhonravov, Basics of Optics of Multilayer Systems, Ed. Frontières, Singapore, 1992.
[12] L. Ward, The Optical Constants of Bulk Materials and Films, Adam Hilger Series in Optics and Optoelectronics, Institute of Physics, Bristol, UK, 1988.
[13] E.D. Palik, Handbook of Optical Constants of Solids, Academic Press, Orlando, FL, 1985.
[14] O.S. Heavens, Optical Properties of Thin Solid Films, Dover, New York, 1965.
[15] Manual of the Shimadzu 3101PC UV–VIS–NIR double beam spectrophotometer.
[16] M. Bass, Handbook of Optics, 2nd edn., McGraw-Hill, New York, 1995.
[17] T.C. Anthony, A.L. Fahrenbruch, R.H. Bube, J. Cryst. Growth 59 (1982) 289.
[18] Y. Laaziz, A. Bennouna, E.L. Ameziane, Solar Energy Mater. Solar Cells 31 (1993) 23.
[19] M. Benmoussa, E. Ibnouelgazi, A. Bennouna, E.L. Ameziane, Thin Solid Films 265 (1996) 22.
[20] M. Benmoussa, E. Ibnouelgazi, A. Bennouna Y. Laaziz, E.L. Ameziane, Le Vide, les Couches Minces 275 (1995) 24.
[21] M.Y. Elazhari, M. Azizan, A. Bennouna, A. Outzourhit, E.L. Ameziane, M. Brunel, Solar Energy Mater. Solar Cells (preprint).
[22] H. Bellakhdar, A. Bennouna, A. Outzourhit, E.L. Ameziane, Solar Energy Mater. Solar Cells (preprint).
[23] H. Mohssine, F. Debbagh, E.L. Ameziane, A. Bennouna, Proc. 3rd World Renewable Energy Congress, Reading, UK, Part 1, Pergamon, Oxford, 1994, p. 205.
[24] A. Yassar, A. Bennouna, M. Khaidar, E.L. Ameziane, G. Horowitz, D. Delabouglise, M. Hmyene, F. Garnier, J. Appl. Phys. 72 (1992) 4873.
[25] E.L. Ameziane, M. Khaïdar, A. Bennouna, A. Abouelaoualim, A. Essafti, Solar Wind Technol. 6 (1989) 569.
[26] P. Fau, J.P. Bonino, A. Rousset, Le Vide, les Couches Minces 49 (1993) 199.
[27] K. Nanbu, T. Morimoto, Y. Goto, JSME Int. J. Ser. B: Fluids Thermo. Eng. 36 (1993) 313.